

## Electronic Supplementary Information

# A double intramolecular cage contraction within a self-assembled metallo-supramolecular bowl

**Boris Brusilowskij, Saskia Neubacher, and Christoph A. Schalley\***

*Institut für Chemie und Biochemie - Organische Chemie, Freie Universität,  
Takustr. 3, D-14195 Berlin, Germany  
email: schalley@chemie.fu-berlin.de*

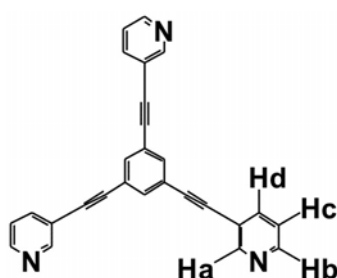
**General:** All chemicals were of reagent grade quality and used as obtained from commercial suppliers without further purification. Solvents were used as received or - if necessary - dried over 4 Å molecular sieve. Pd(dppp)OTf<sub>2</sub> and Pt(dppp)OTf<sub>2</sub> were prepared as described in literature<sup>1</sup>.

**Instrumentation and methods:** <sup>1</sup>H, <sup>31</sup>P, and *H,H* COSY NMR spectra were recorded with Bruker ECX 400 or Jeol Eclipse 500 instruments. All chemical shifts are reported in ppm with solvent signals taken as internal standards; coupling constants are in Hz. The electrospray-ionization Fourier-transform ion-cyclotron-resonance (ESI-FTICR) mass spectrometric experiments were performed with a Varian/IonSpec QFT-7 FTICR mass spectrometer equipped with a superconducting 7 Tesla magnet and a micromass Z-spray ESI ion source utilizing a stainless steel capillary with a 0.65 mm inner diameter. The sample solutions were introduced into the source with a syringe pump (Harvard Apparatus) at a flow rate of ca. 2.0 μL·min<sup>-1</sup>. Parameters were adjusted as follows: Source temperature: 40 °C; temperature of desolvation gas: 40 °C; parameters for capillary voltage, sample and extractor cone voltages are optimized for maximum intensities. No nebulizer gas was used for the experiments. The ions were accumulated in the instrument's hexapole for 2 to 5 s. Next, the ions were transferred into the FTICR analyzer cell by a quadrupole ion guide. The FTICR cell was operated at pressures below 10<sup>-9</sup> mbar, and detected by a standard excitation and detection sequence. For tandem mass spectrometric experiments, the ions of interest were mass-selected and subsequently vibrationally excited for 1,000 ms with a CO<sub>2</sub> laser in the IR region (infrared multiphoton dissociation (IRMPD); 10.6 μm wavelength) to induce fragmentation. The maximum laser power is 25 W and can

be controlled by the instrument in percentages of 25 W. MS<sup>3</sup> experiments were performed with the same sequence of steps which was just extended by a second mass-selection of one of the fragment ions and a second laser pulse to induce fragmentation of that ion. For each measurement, 20 to 40 scans were averaged to improve the signal-to-noise ratio.

## Synthesis of ligand 1

### 1,3,5-tris(pyridin-3-ylethynyl)benzene



3-Iodopyridine (212.6 mg, 1.032 mmol) and 1,3,5-triethynylbenzene (50.0 mg, 0.333 mmol) were dissolved under argon atmosphere in 10 ml DMF. After the addition of triethylamine (1.5 ml), Pd(PPh<sub>3</sub>)<sub>2</sub>Cl<sub>2</sub> (35.1 mg, 0.049 mmol), PPh<sub>3</sub> (26.2 mg, 0.099 mmol), and CuI (9.5 mg, 0.049 mmol), the reaction mixture was stirred for 24 h at r.t. The solvent was evaporated under reduced pressure, the remaining residue was re-dissolved in CH<sub>2</sub>Cl<sub>2</sub> (5 ml) and washed 3 times with H<sub>2</sub>O (100 ml). After evaporation of the solvent under reduced pressure, the crude product was purified by column chromatography (silica gel, mobile phase: CH<sub>2</sub>Cl<sub>2</sub>/ EtOH = 98 : 2). Yield: 62.0 mg, 49%. <sup>1</sup>H NMR: (400 MHz, CDCl<sub>3</sub>): δ = 7.29 (ddd, <sup>3</sup>J = 7.90 Hz <sup>3</sup>J = 4.90 Hz, <sup>5</sup>J = 0.8 Hz, 3H; py-H<sub>c</sub>), 7.70 (s, 3H; Ar-H), 7.80 (ddd, <sup>3</sup>J = 7.90, <sup>4</sup>J = 1.78 Hz, <sup>4</sup>J = 2.05 Hz, 3H; py-H<sub>d</sub>), 8.57 (dd, <sup>3</sup>J = 4.90 Hz <sup>4</sup>J = 1.66 Hz, 3H; py-H<sub>b</sub>), 8.77 (d, <sup>4</sup>J = 1.4 Hz, 3H; py-H<sub>a</sub>); <sup>13</sup>C-NMR (125 MHz, CDCl<sub>3</sub>): δ = 87.56, 90.71 (C≡C), 119.91, 123.20 (C<sub>q</sub>), 123.71, 134.64, 138.61, 149.14, 152.43 (Ar-CH); ESI-MS: *m/z* (%) = 382.12 ([M+H]<sup>+</sup>, 100%)

### Preparation of the Pd and Pt assemblies as their triflate salts

The assemblies were prepared by stirring a 1:1.5 ratio of **1** and **2a** or **2b** in dichloromethane at r.t. The reactions were monitored by <sup>31</sup>P{<sup>1</sup>H} NMR which allowed us to follow the consumption of 'free' corner upon product formation.

**Pd assembly:** ligand **1** (19.6 mg, 0.051 mmol) in dichloromethane (5 ml) was added to a suspension of Pd(dppp)OTf<sub>2</sub> (**2a**) (62.90 mg, 0.070 mmol) in dichloromethane (5 ml). The mixture was stirred at r.t. under nitrogen for 3 d. The addition of diethyl ether led to the precipitation of the product as a white-yellowish powder. <sup>31</sup>P NMR (200 MHz, DMF-*d*<sub>7</sub>): δ = 13.90 (br), 9.12 (br) ppm. <sup>31</sup>P NMR (200 MHz, DMSO-*d*<sub>6</sub>): δ = 15.42 (br), 9.08 (br) ppm. <sup>31</sup>P NMR (200 MHz, nitrobenzene-*d*<sub>5</sub>): δ = 8.91 (s), 8.53 (s), 7.90 (s) ppm. ESI-MS *m/z* = 922 ([M<sub>3</sub>L<sub>2</sub>-OTf]<sup>3+</sup>, 100%), 1458 ([M<sub>3</sub>L<sub>2</sub>-OTf]<sup>2+</sup>, 25%), 1993 ([M<sub>4</sub>L<sub>6</sub>-3OTf]<sup>3+</sup>, 5%), 3064 ([M<sub>3</sub>L<sub>2</sub>-OTf]<sup>+</sup>, 1%).

**Pt assembly:** ligand **1** (10.1 mg, 0.026 mmol) in dichloromethane (5 ml) was added to a suspension of Pt(dppp)OTf<sub>2</sub> (**2b**) (35.5 mg, 0.039 mmol) in dichloromethane (5 ml). The mixture was stirred at r.t. under nitrogen for 10 d. The addition of diethyl ether led to the precipitation of the product as a white powder. <sup>31</sup>P-NMR (200 MHz, nitrobenzene-*d*<sub>5</sub>): -14.47 (br) (<sup>1</sup>J<sub>(Pt-P)</sub> = 3034 Hz); ppm. ESI -MS: *m/z* = 1591 ([M<sub>3</sub>L<sub>2</sub>-OTf]<sup>3+</sup>, 100%).

### **<sup>1</sup>H NMR spectra**

The <sup>1</sup>H NMR spectra show the ortho-pyridine H<sub>a</sub> and H<sub>b</sub> hydrogens to undergo significant complexation-induced shifts (see below). Due to strong signal overlap and signal broadening, a straight-forward signal assignment is however difficult to achieve. We therefore refrain from providing <sup>1</sup>H NMR data here.

## $^1\text{H}, ^1\text{H}$ COSY NMR spectra

With  $^1\text{H}, ^1\text{H}$  COSY NMR experiments, the  $\text{H}_a$  and  $\text{H}_b$  signals can be distinguished through the cross peaks that indicate a coupling of  $\text{H}_b$  and  $\text{H}_c$ .  $\text{H}_a$  does not couple and thus no cross peaks are observed.

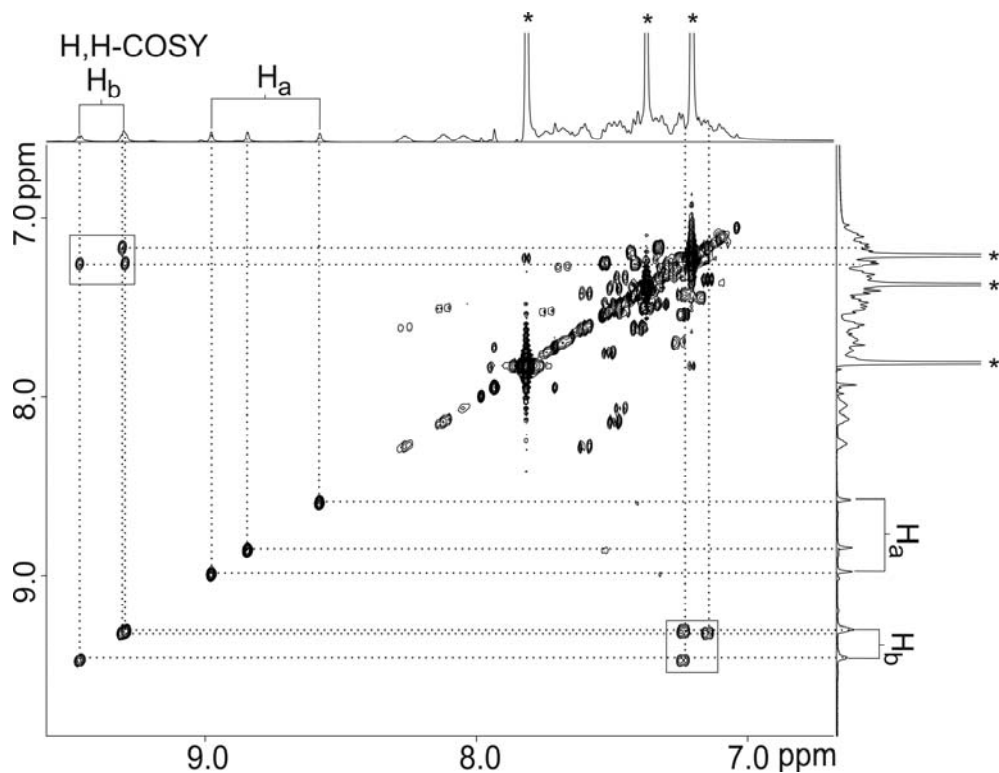


Figure S1:  $\text{H}, \text{H}$ -COSY spectrum of the aromatic region of **1** and **2a** in nitrobenzene- $\text{d}_5$  (\*). Through the coupling with other protons, the two pyridine protons adjacent to the nitrogen can be unambiguously identified.

### Variable temperature $^1\text{H}$ and $^{31}\text{P}$ NMR experiments

Variable-temperature  $^1\text{H}$  and  $^{31}\text{P}$  NMR spectra in nitrobenzene- $d_5$  show a fast exchange of ligand **1** between the two assemblies at higher temperatures. Since several different exchange processes may contribute, no clear coalescence temperature can be defined. Qualitatively, however, the fast exchange is indicated by the presence of only one signal in the  $^{31}\text{P}$  NMR spectrum at 408 K.

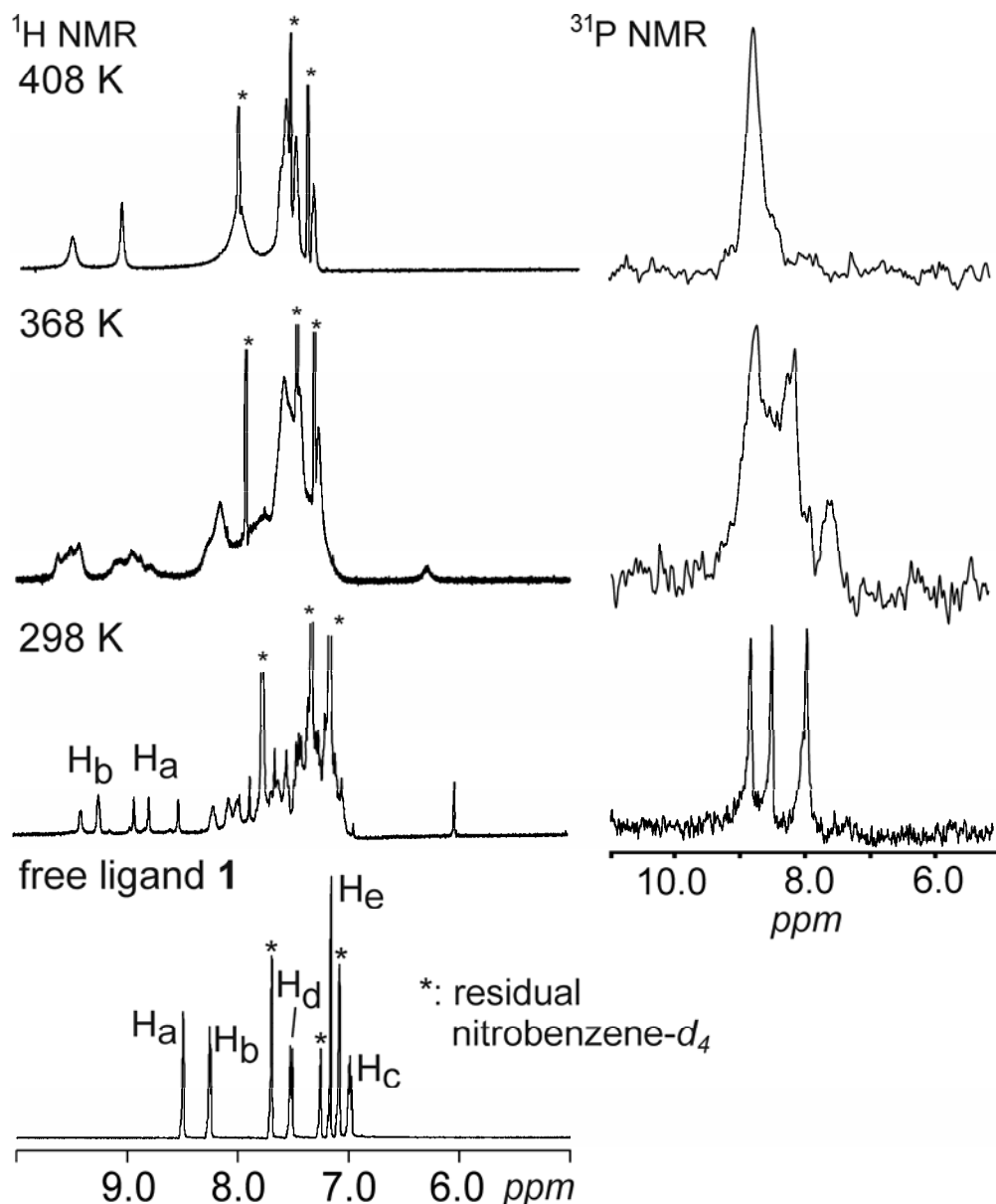


Figure S2: Selected temperature-dependent  $^1\text{H}$  NMR (aromatic region) and  $^{31}\text{P}$  NMR spectra of the mixture **1** and **2a** in nitrobenzene- $d_5$  ( $[\mathbf{2a}] = 5 \text{ mmol}$ , the temperature is raised from bottom to the top). For comparison, the  $^1\text{H}$  NMR spectrum of the free ligand in nitrobenzene- $d_5$  is shown. Clearly,  $\text{H}_a$  and  $\text{H}_b$  experience complexation-induced shifts, when the assemblies form.

### <sup>31</sup>P NMR Spectra of the 3a/4a Equilibrium in More Competitive Solvents

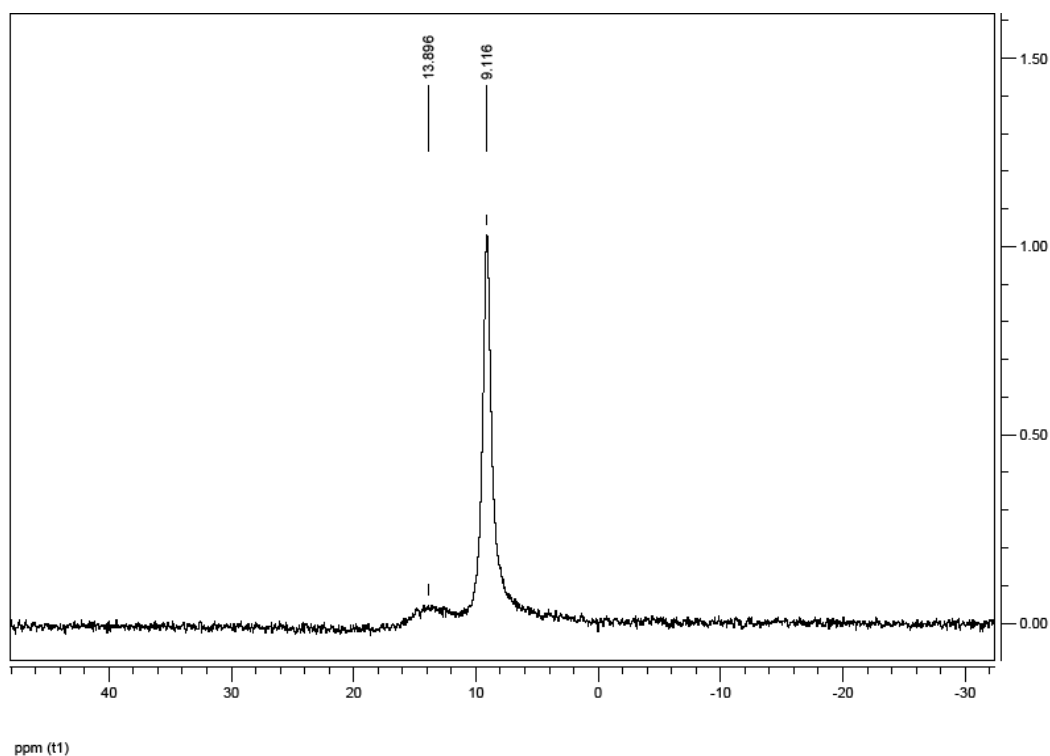


Figure S3: <sup>31</sup>P NMR spectrum of **1** and **2a** in a 1:1.5 ratio (DMF-d<sub>7</sub>, 25 °C, [**2a**] 5mmol).

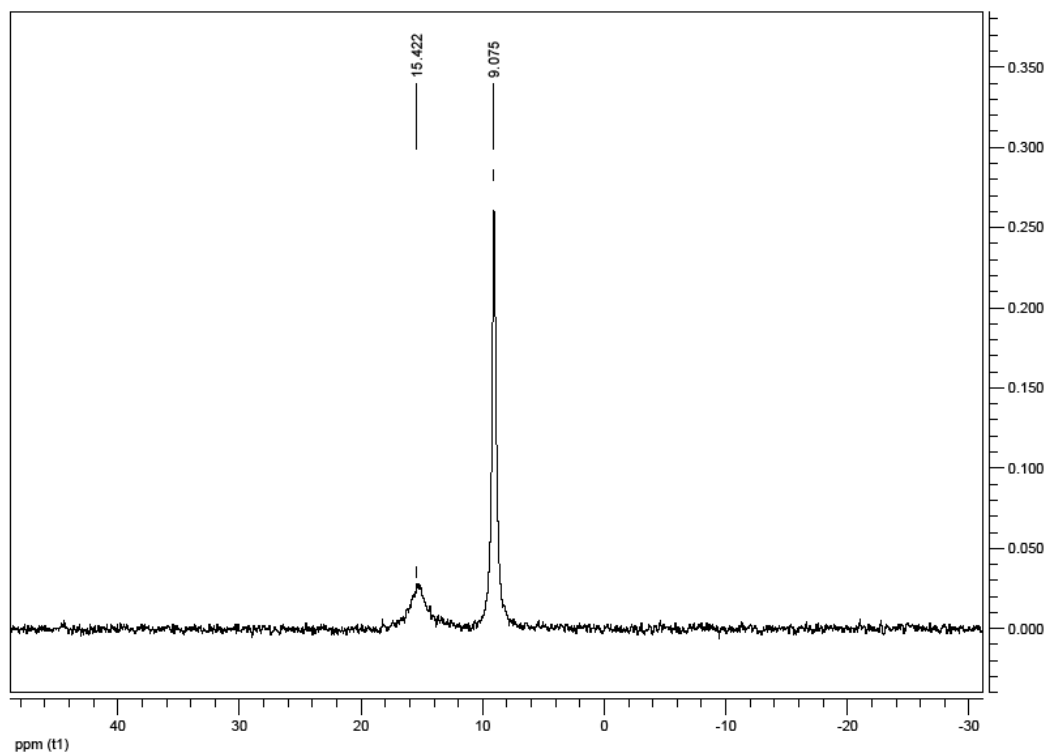


Figure S4: <sup>31</sup>P NMR spectrum of **1** and **2a** in a 1:1.5 ratio (DMSO-d<sub>6</sub>, 25 °C, [**2a**] 5mmol).

### $^{31}\text{P}$ NMR Spectrum of **3b**

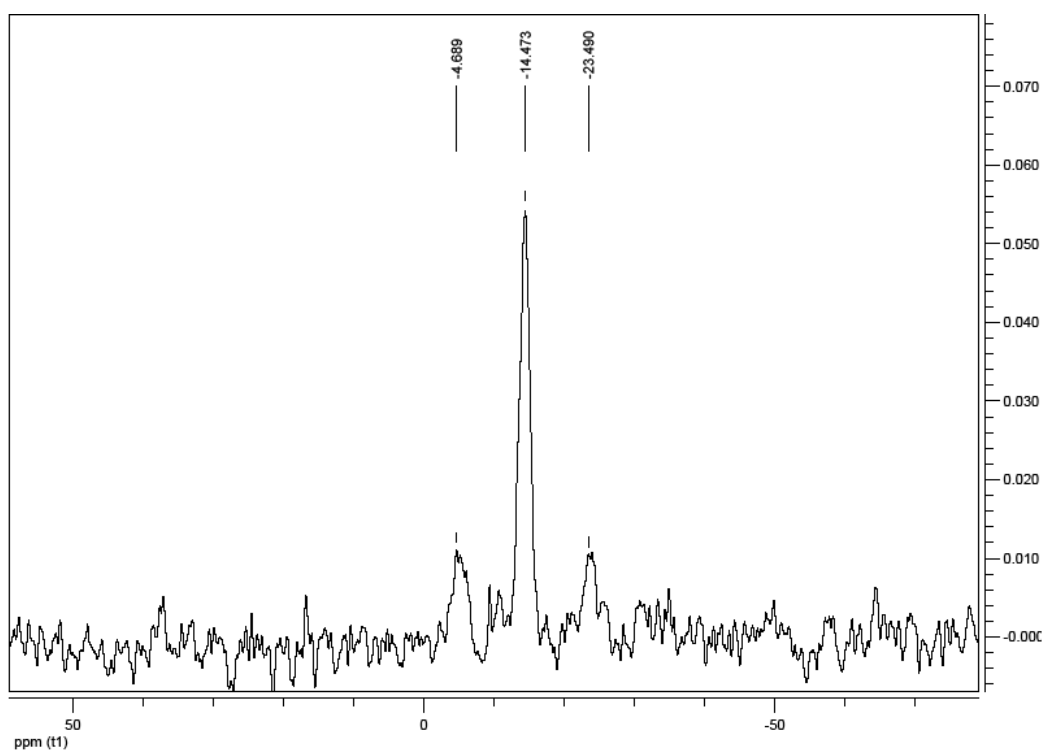


Figure S5:  $^{31}\text{P}$  NMR spectrum of **1** with **2b** in a 1:1.5 ratio (nitrobenzene- $d_5$ , 25 °C, [**2b**] = 5mmol). The  $P$ - $^{195}\text{Pt}$  coupling constant is 3034 Hz, a value which is much lower than that of the corresponding precursor complex (3650 Hz). The coupling constant is a very sensitive indicator of pyridine complexation and thus confirms the formation of an assembly.

## Mass spectrometry studies:

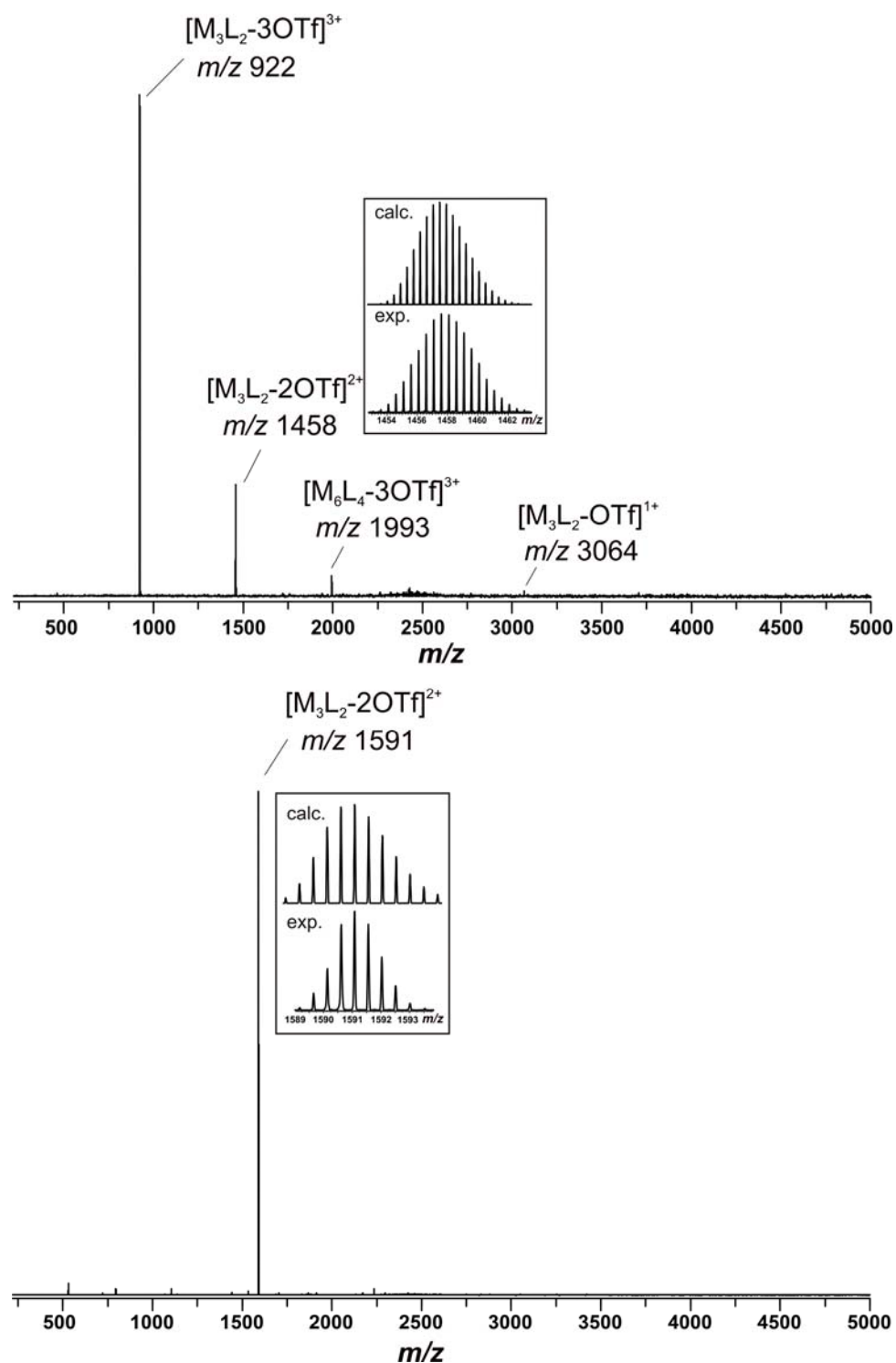


Figure S6: ESI-FTICR-MS spectra of the Pd (Top) and the Pt (bottom) assemblies in  $CH_2Cl_2/MeOH$  (1:100). The insets show the isotope patterns of the doubly charged  $M_3L_2$  assemblies and compare them to the calculated isotopic distribution.



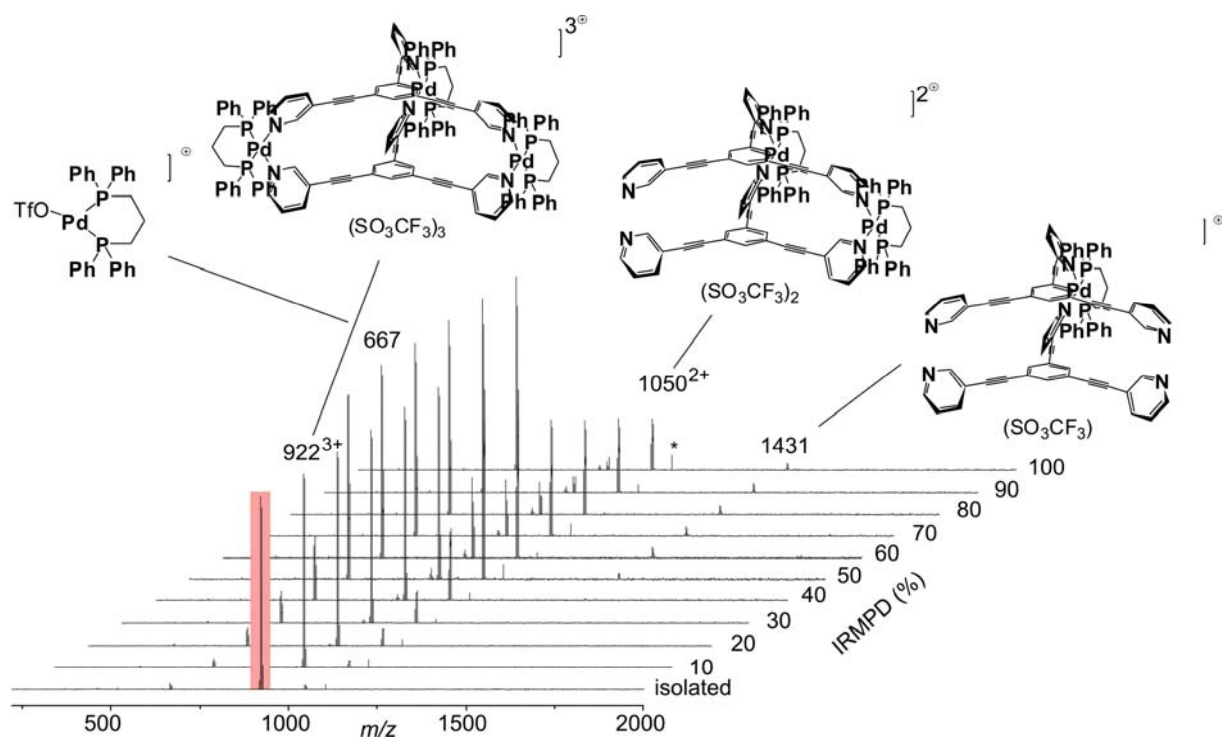


Figure S7: Tandem mass spectra of mass-selected triply charged Pd assembly (red) (with increasing the IRMPD laser intensity from the bottom to the top, \* = artefact due to stray radiation).

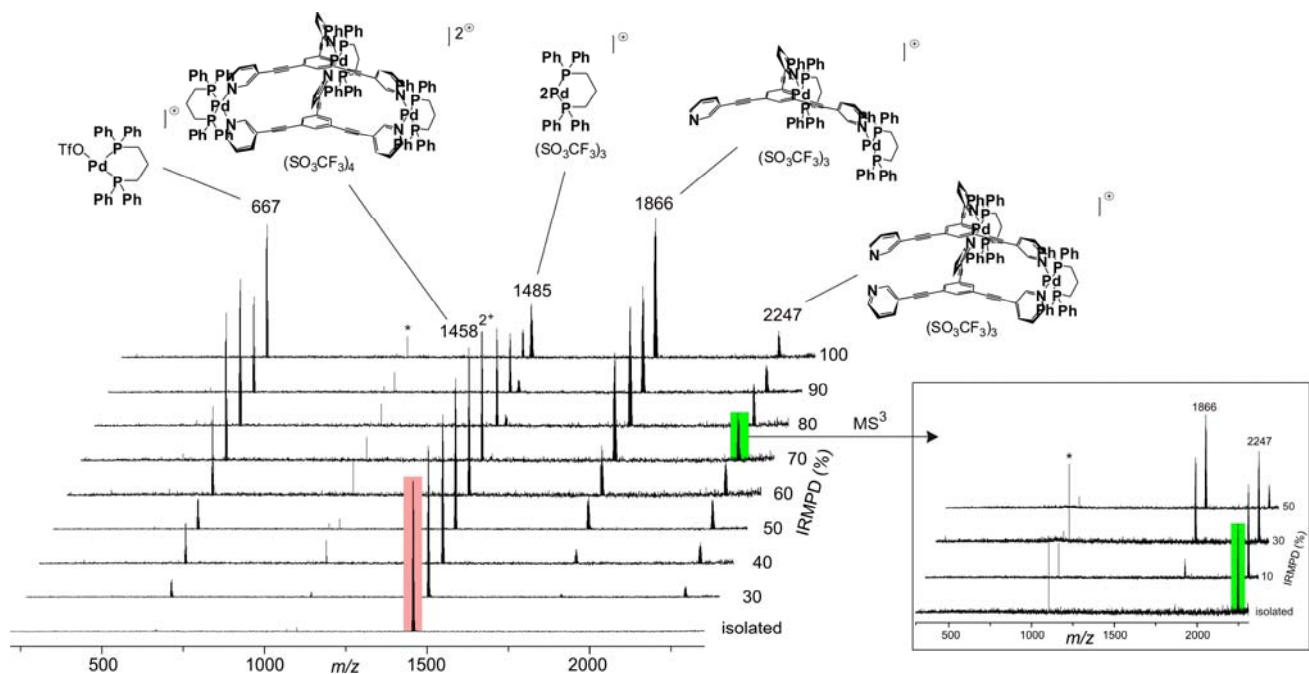


Figure S8: Tandem mass spectra of mass-selected doubly charged Pd assembly (red) ( $MS^2$  experiment (left) and  $MS^3$  experiment (right), with increasing the IRMPD laser intensity from the bottom to the top, \* = artefact due to stray radiation).

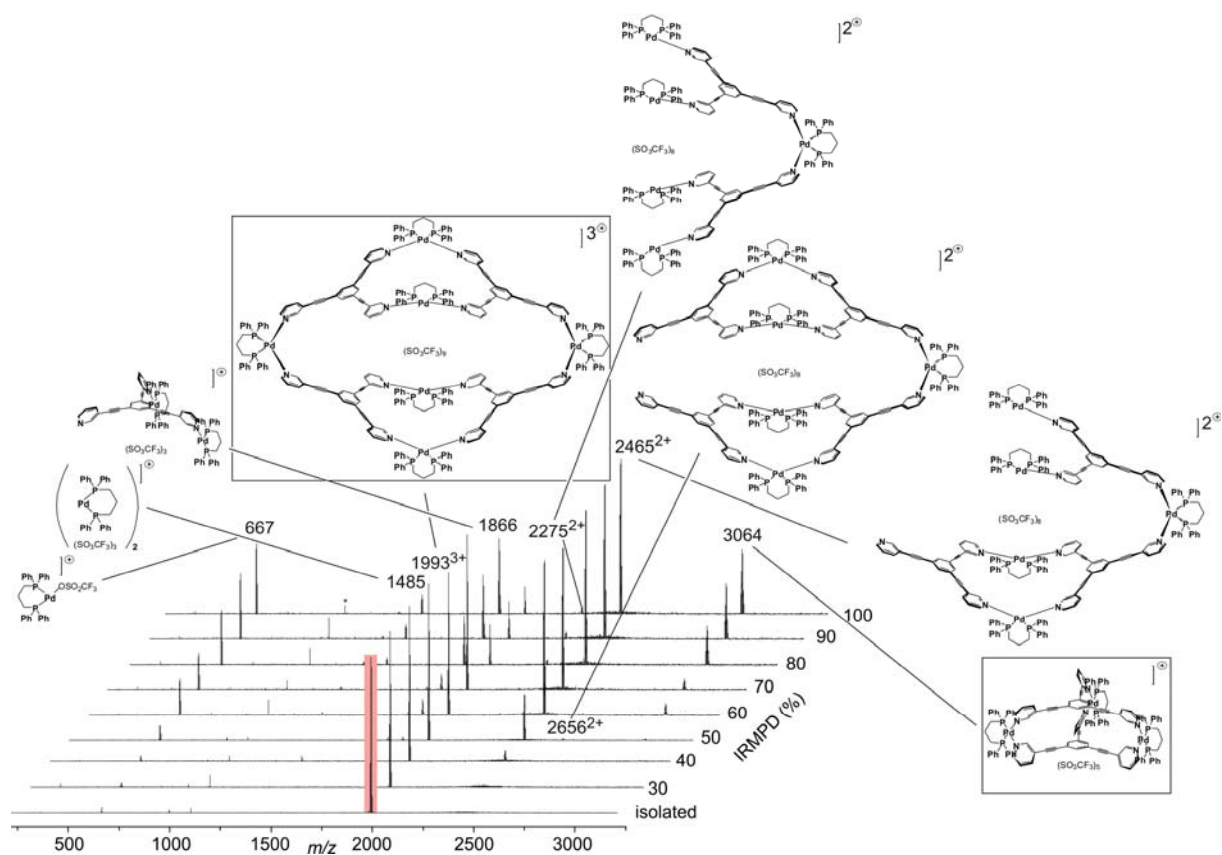


Figure S9: Tandem mass spectra of mass-selected triply charged Pd assembly (red) (with increasing the IRMPD laser intensity from the bottom to the top, \* = artefact due to stray radiation).

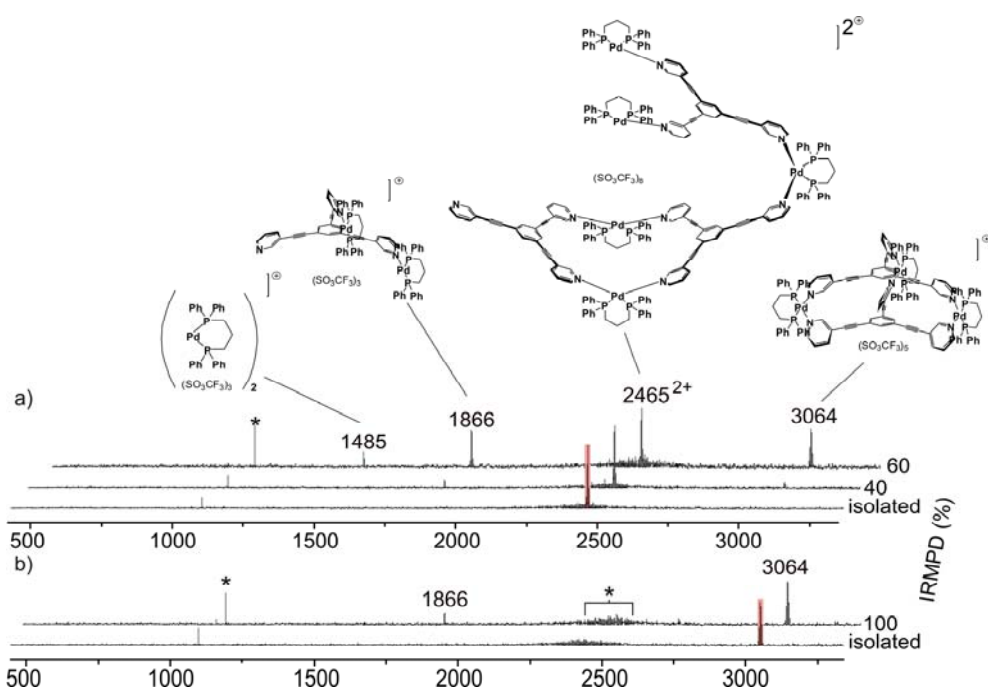


Figure S10:  $MS^3$  experiments after mass selection of; a) doubly charged 2465-ion (red) and b) singly charged 3064-ion (red) (with increasing the IRMPD laser intensity from the bottom to the top, \* = artefact due to stray radiation).

## Molecular Modelling

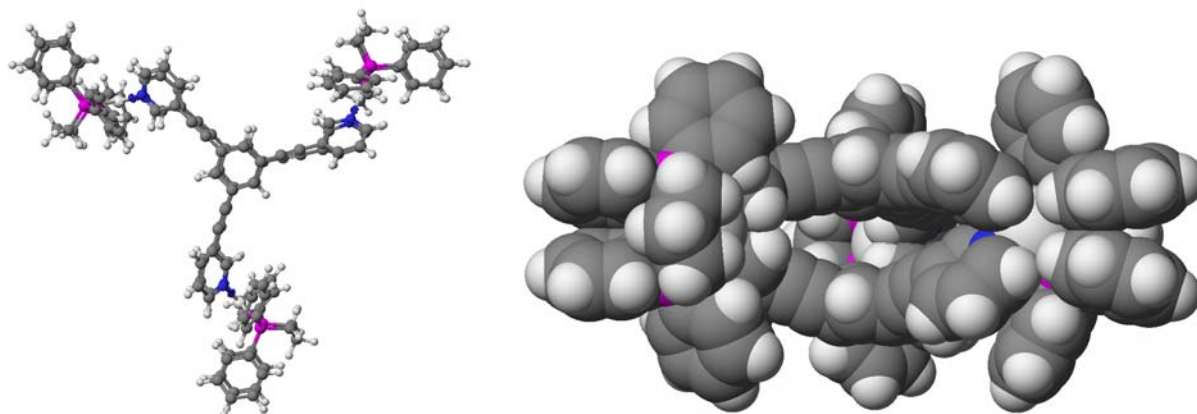


Figure S11: Molecular Modelling (using CAChe, MM2)<sup>2</sup> of the molecular cage on the left represented as ball and cylinder (view from the top) and on the right as space filling (view from the side) model.

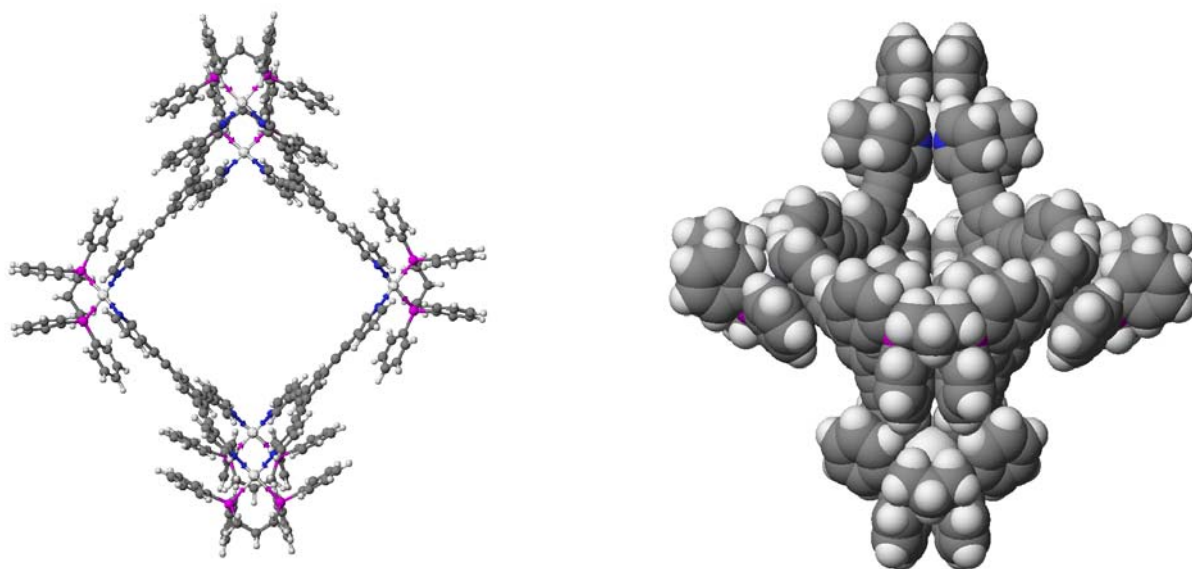


Figure S12: Molecular Modelling (using CAChe, MM2) of the molecular bowl on the left represented as ball and cylinder (view from the top) and on the right as space filling (view from the side) model.

<sup>1</sup> P. J. Stang, D. H. Cao, *J. Am. Chem. Soc.* 1994, **116**, 4981-4982.

<sup>2</sup> Cache Program Package, Fujitsu Ltd., Krakow Poland